SAR Studies of Dihydro-*β*-agarofuran Sesquiterpenes as Inhibitors of the Multidrug-Resistance Phenotype in a *Leishmania tropica* Line Overexpressing a P-Glycoprotein-Like Transporter

Fernando Cortés-Selva,[†] Mercedes Campillo,[‡] Carolina P. Reyes,[§] Ignacio A. Jiménez,[§] Santiago Castanys,[†] Isabel L. Bazzocchi,[§] Leonardo Pardo,*[,‡] Francisco Gamarro,*[,†] and Angel G. Ravelo*[,§]

Instituto de Parasitología y Biomedicina "López-Neyra", Consejo Superior de Investigaciones Científicas, c/Ventanilla 11, 18001 Granada, Spain, Laboratori de Medicina Computacional, Unitat de Bioestadistica, Institut de Neurociències, Universitat Autònoma de Barcelona, 08193 Cerdanyola del Vallès, Barcelona, Spain, and Instituto Universitario de Bio-Orgánica "Antonio González", Universidad de La Laguna, Avenida Astrofísico Francisco Sánchez, 2, 38206 La Laguna, Tenerife, Spain

Received July 23, 2003

A series of dihydro-*β*-agarofuran sesquiterpenes isolated from the leaves of *Maytenus cuzcoina* (**1**−**10**) or semisynthetic derivatives (**11**−**30**) have been tested on a multidrug-resistant *Leishmania tropica* line overexpressing a P-glycoprotein-like transporter to determine their ability to revert the resistance phenotype and to modulate intracellular drug accumulation. Almost all natural compounds showed potent reversal activity with different degrees of selectivity. Compounds **2**, **7**, and **8** are the most effective reversal agents tested against the multidrug resistance phenotype of *Leishmania*. Three-dimensional quantitative structure−activity relationships using the comparative molecular similarity indices analysis (CoMSIA) were employed to characterize the steric (contribution of 5.4%), electrostatic (58.9%), lipophilic (10.0%), and hydrogen-bond-donor (13.3%) and -acceptor (7.5%) requirements of these sesquiterpenes as modulators at the P-glycoprotein-like transporter. The most salient features of these requirements are the H-bond interaction between the substituents at the C-2 and C-6 positions with the receptor.

Introduction

Natural products play important roles in both drug discovery and chemical biology. In fact, many approved therapeutics as well as drug candidates are derived from natural sources. Additionally, natural products have been extensively used to elucidate complex cellular mechanisms, including signal transduction and cell cycle regulation, leading to the identification of important targets for therapeutic intervention. As a result of recent advances in biology, there is now an increased demand for new natural product-like small molecules. Specifically, the fields of genomics and proteomics promise the rapid identification of a large numbers of gene products for which small molecule modulators will be of both biological and medicinal interest.[1]

Over the last 30 years, a large number of secondary metabolites exhibiting a wide range of bioactivity have been isolated from Celastraceae, the sesquiterpenes being the most widespread and characteristic metabolites of this family. Generally, they occur as polyesters of variously polyoxygenated tricyclic scaffolds, all based on a core C_{15} skeleton known as dihydro-*β*-agarofuran [5,11-epoxy-5*β*,10α-eusdesm-4(14)-ene], and they are considered to be chemotaxonomic indicators of the family. X-ray data and conformational studies using molecular mechanics procedures showed that the *trans*-fused A and B rings formed a trans chair−chair decalin system, slightly distorted by the presence of the 1,3-diaxial bond responsible for the tetrahydrofuran C ring, practically perpendicular to the plane formed by carbons C-5, C-7, C-8, and C-10 (Figure 1).[2]

The interest generated by sesquiterpenes from Celastraceae has increased in line with the complexity of the substances isolated and, more importantly, with their wide range of biological actions, suggesting that derivatives of this sesquiterpene motif may be capable of interacting with a variety of cellular targets. Recently, sesquiterpenes have shown immunosuppressive,[3] anti-HIV,[4] reversal of multidrug resistance (MDR) phenotype,[5,6] and antitumor-promoting activities.[7] In addition, the fact that many of the compounds are active in cell-based assays suggested that products with a dihydro-*β*-agarofuran unit remain sufficiently lipophilic to cross cell membranes, a key feature of any biologically relevant compound. On the basis of the biological and structural properties, we propose the selection of sesquiterpene polyesters with a dihydro-*β*-agarofuran skeleton as a *privileged structure*. This term describes selected structural types, like polycyclic heteroatomic systems, capable of orienting varied substituent patterns in a well-defined three-dimensional space and bind to multiple, unrelated classes of protein receptors as high-affinity ligands.[8]

Drug resistance has emerged in the last years as one of the major impediments for the treatment of diseases produced by protozoan parasites. ABC (ATP-binding cassette) transporters are involved, at least in vitro, in

* Corresponding authors. L.P.: tel, 34-93-5812797; fax, 34-93-5812344; e-mail, leonardo.pardo@uab.es. F.G.: tel, 34-958-805185; fax, 34-958-203323; e-mail, gamarro@ipb.csic.es. A.G.R.: tel, 34-922-318576; fax, 34-922-318571; e-mail, agravelo@ull.es.
[†] Consejo Superior de Investigaciones Científicas.
[‡] Universitat Autònoma de Barcelona.
[§] Universidad de La Laguna.

10.1021/jm0309699 CCC: $27.50
Published on Web 12/30/2003

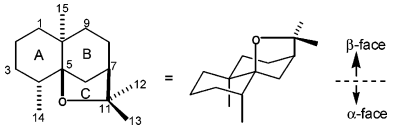

Figure 1. Dihydro-β-agarofuran skeleton.

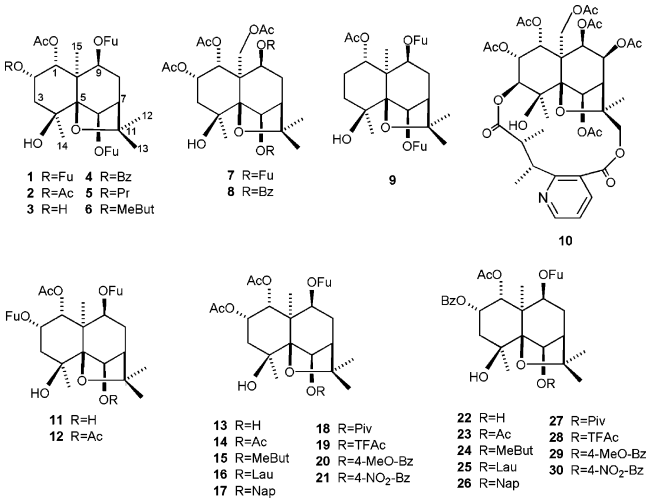

Figure 2. Sesquiterpenes assayed for the chemosensitization of a MDR *L. tropica* line.

the resistance to many antiparasitic drugs.[6,9−11] In addition, new putative antiparasitic drugs such as anthracyclines,[12] taxol,[13] or azoles,[14,15] are known substrates of ABC transporters, and thus could induce an MDR phenotype. One ABC transporter homologous to the human MDR-P-glycoprotein (Pgp) confers an MDR phenotype in *Leishmania*[6,11,16] similar to that characterized in cancer cells. Moreover, *Leishmania* Pgp also confers resistance against alkyllysophospholipids, such as miltefosine, the most promising leishmanicidal agent.[6] Therefore, the development of inhibitors of these transporters is of high clinical relevance. The main difference between the MDR phenotypes conferred by Pgp in mammalian cells and the Pgp-like transporter in *Leishmania* is the absence of significant reversal effects by classical Pgp inhibitors such as verapamil, among others.[11] This observation led us to explore new inhibitors against this protein. Agarofuran sesquiterpenes are new, promising reversal agents; they have efficiently overcome the MDR phenotype in *Leishmania*,[5,6,17] including resistance to alkyllysophospholipids, probably due to their binding to the transmembrane domains of the *Leishmania* Pgp-like transporter and blocking drug efflux.

As a part of an intensive investigation into active metabolites as reversal agents of MDR phenotype, we describe in this paper the biological evaluation as modulators of the MDR phenotype of a *Leishmania tropica* line and a three-dimensional quantitative structure−affinity relationship analysis (3D-QSAR)[18] of 30 (**1**−**30**) sesquiterpenes with a dihydro-β-agarofuran skeleton (Figure 2), among them 10 (**1**−**10**) that were isolated from *Maytenus cuzcoina*[7] and 20 semisynthetic derivatives (**11**−**30**) not previously described. The 3D-QSAR was performed using an extension of the CoMFA methodology,[19,20] the comparative molecular similarity indices analysis (CoMSIA).[21] This methodology was applied to these sesquiterpenes bearing substituents at the C-2, C-6, C-9, and C-15 positions of the dihydro-β-agarofuran skeleton, to characterize the steric, electrostatic, hydrophobic, and hydrogen-bond-donor and -acceptor requirements needed at the active sites of the receptors for ligand recognition. One of the unique features of CoMFA is its ability to represent the 3D-QSAR model in terms of color contour maps that depict locations on the ligands where structural modifications might enhance their biological activity (e.g. binding affinity). These maps can serve as a guide when designing analogues within the same series of compounds that possess desirable biological properties.

Methods

3D-QSAR/CoMSIA Method. The equilibrium structures of the sesquiterpenes were obtained by full ab initio geometry optimization with the 3-21G basis set. A critical step in CoMSIA is to select a proper alignment rule. The entire set of sesquiterpene analogues was oriented in space by superimposing the common and rigid dihydro-β-agarofuran skeleton. The percentage of inhibition in both MDR and wild-type (WT) parasites is a function of both the stabilization of the complexes between the ligand molecules and the protein receptor and the solvation energy of the ligands. Thus, the QSAR Tables 3 and 4 consist the percentage of inhibition values (dependent variable) and the electrostatic, steric, hydrophobic, and hydrogen-donor and hydrogen-acceptor fields (independent variables), to mimic the stabilization energy of the receptor−ligand complex, and the solvation energy (independent variable). The atom-centered atomic charges used in CoMSIA to evaluate the electrostatic contributions were computed from the molecular electrostatic potential[22] using 6-31G* basis set, a common procedure for the simulation of proteins, nucleic acids, and organic molecules.[23] Solvation free energies (ΔG_{solv}) of sesquiterpenes were calculated with the PM3-SR5.42R procedure within the AMSOL 6.7.2 program.[24] The potential fields were calculated at each lattice intersection of a regularly spaced grid of 2 Å. A sp^3 carbon atom with a van der Waals radius of 1.52 Å carrying a charge of +1.0 served as a probe atom to calculated the fields with an attenuation factor of 0.3.[25] Partial least squares (PLS) analysis[26−29] was used to derive linear equations from the resulting matrixes. Leave one out (LOO) cross-validation was employed to select the number of principal components and to calculate the cross-validated statistics. The final CoMSIA model was generated using non-cross-validation and the number of components suggested by the LOO validation run. The 3D-QSAR/CoMSIA study was carried out with the QSAR module of the SYBYL 6.6 program,[30] using default parameters. All the quantum mechanical calculations were performed with the Gaussian 98 system of programs.[31]

Results and Discussion

The products considered for biological investigation (Figure 2) were isolated from *M. cuzcoina* (compounds **1**−**10**[7]) or prepared by standard methods (compounds **11**−**30**), as described in Scheme 1.

Compounds **11**, **13**, and **22** (Figure 2) were prepared by partial basic hydrolysis of **1**, **2**, and **4**, respectively.

Table 1. Effect of Sesquiterpenes on the Growth of WT and MDR *L. tropica* Lines

	growth inhibition[a] (%)							
	15 μM		7 μM		3 μM		1 μM	
compd	WT	MDR	WT	MDR	WT	MDR	WT	MDR
1	23.4 ± 3.1	93.5 ± 1.7	18.1 ± 6.4	86.2 ± 0.2	13.8 ± 4.9	52.9 ± 10.1	–[b]	10.0 ± 9.8
2	15.2 ± 3.5	94.4 ± 1.8	9.7 ± 6.5	90.9 ± 2.1	–	83.5 ± 9.2	–	24.5 ± 0.7
3	–	28.7 ± 8.1	–	9.1 ± 6.3	–	–	–	–
4	35.3 ± 5.8	92.7 ± 5.5	21.4 ± 8.6	93.7 ± 1.5	16.5 ± 4.1	74.8 ± 5.9	–	11.7 ± 4.7
5	26.8 ± 2.9	95.8 ± 1.6	20.6 ± 2.5	94.8 ± 4.5	15.9 ± 5.7	89.1 ± 3.4	–	30.3 ± 2.5
6	31.5 ± 6.2	94.7 ± 2.5	24.9 ± 8.0	92.0 ± 1.6	21.8 ± 7.7	87.6 ± 3.8	–	25.7 ± 7.5
7	7.2 ± 6.0	94.3 ± 3.0	–	89.5 ± 2.0	–	79.6 ± 6.8	–	25.7 ± 7.6
8	15.2 ± 5.6	90.9 ± 5.0	11.0 ± 6.6	89.9 ± 5.2	6.9 ± 6.9	77.5 ± 5.0	–	18.0 ± 7.1
9	24.6 ± 7.1	89.9 ± 4.8	16.4 ± 4.9	89.0 ± 1.3	14.8 ± 2.8	66.9 ± 9.9	–	20.3 ± 5.1
10	–	–	–	–	–	–	–	–
11	–	44.5 ± 2.1	–	28.5 ± 13.4	–	–	–	–
12	–	–	–	–	–	–	–	–
13	–	10.9 ± 7.9	–	–	–	–	–	–
14	–	50.6 ± 9.3	–	17.1 ± 6.7	–	–	–	–
15	–	–	–	–	–	–	–	–
16	–	80.5 ± 4.5	–	29.2 ± 10.6	–	8.8 ± 1.3	–	–
17	10.6 ± 0.6	95.2 ± 1.3	–	50.7 ± 8.5	–	16.5 ± 8.8	–	–
18	–	96.7 ± 0.0	–	82.5 ± 5.9	–	44.5 ± 1.0	–	18.1 ± 7.4
19	–	7.1 ± 2.7	–	–	–	–	–	–
20	17.2 ± 0.6	98.4 ± 0.7	–	85.0 ± 3.2	–	35.4 ± 8.6	–	11.9 ± 6.7
21	–	59.5 ± 2.8	–	15.5 ± 3.0	–	–	–	–
22	8.0 ± 4.6	81.9 ± 3.3	–	41.1 ± 6.7	–	11.1 ± 9.1	–	–
23	–	45.0 ± 5.2	–	14.3 ± 7.3	–	–	–	–
24	–	28.0 ± 9.2	–	10.4 ± 6.3	–	–	–	–
25	–	9.2 ± 4.2	–	–	–	–	–	–
26	–	8.6 ± 3.5	–	–	–	–	–	–
27	–	77.6 ± 4.5	–	25.9 ± 3.5	–	11.2 ± 4.7	–	–
28	–	36.9 ± 4.6	–	9.7 ± 2.3	–	–	–	–
29	–	11.8 ± 0.7	–	–	–	–	–	–
30	10.8 ± 2.5	51.1 ± 4.1	–	26.4 ± 1.3	–	13.5 ± 4.4	–	6.4 ± 3.7

[a] WT and MDR parasites were exposed to 15, 7, 3, and 1 μM of different sesquiterpenes, in the absence or presence of 150 μM DNM, respectively. The results are expressed as percentage of growth inhibition relative to control growth in the absence of sesquiterpene. The data shown are the average of three independent experiments ±SD. [b] Growth inhibition values between 0 and 6% are indicated by a dash for simplicity.

Table 2. Effect of Sesquiterpenes **2**, **7**, and **8** on IC_{50} Values for DNM in a MDR *L. tropica* Line

	MDR							WT
	7 μM			15 μM				
	2	**7**	**8**	**2**	**7**	**8**	c	c
IC_{50}[a] (μM)	30.0 ± 3.6	33.3 ± 9.8	39.0 ± 6.0	9.0 ± 1.4	11.0 ± 2.8	20.0 ± 4.2	290 ± 24.8	3.8 ± 0.9
RI[b]	7.8	8.7	10.2	2.3	2.9	5.2	75.5	1

[a] Parasites were exposed to increasing concentrations of DNM in the presence or in the absence of two different concentrations (7 and 15 μM) of sesquiterpenes. The results are expressed as the concentration of DNM necessary to inhibit the parasites growth by 50%. The data shown are the average of three independent experiments ±SD. [b] Resistance index. Ratio among IC_{50} of the MDR line and IC_{50} of the WT line. [c] No sesquiterpenes were used.

The furoyl group at C-6 was regioselectively cleaved with 0.1 M $NaHCO_3$ without affecting the other esters. The corresponding esters **12**, **14**–**21**, and **23**–**30** were prepared by treatment of **11**, **13**, and **22** with appropriate acyl chloride or anhydride. Due to the dissimilar reactivity of acylating reagents, different reaction conditions were adopted. The structures of compounds **11**–**30** were elucidated by spectroscopic data. Thus, the ^1H NMR spectrum of compound **11** indicated it is the 6-defuroyl derivative of **1**, since the signal of the H-6 proton was shifted from δ 5.43 in **1**[7] to δ 4.56 in **11** and the signals for the aromatic protons of the furoyl group at δ 6.83, 7.44, and 8.18 were not observed. In the same way, the structures of compounds **13** and **22** were determined as the 6-defuroyl derivative of **2** and **4**, respectively. Spectroscopic data showed that compound **12** is the 6-acetyl derivative of **11**, because of the presence of an additional acetate methyl signal at δ 2.14 and the fact that the signal of the H-6 proton was shifted from δ 4.56 in **11** to δ 5.61 in **12**. The structures of compounds **14**–**21** and **23**–**30** were determined in a similar manner.

The reversal effects of dihydro-β-agarofuran sesquiterpenes **1**–**30** in an MDR *L. tropica* line grown in the presence of daunomycin (DNM) were studied by using an MTT-based assay. Their intrinsic cytotoxicity was determined by using the same concentration of modulators in both parental WT (Table 1) and MDR parasites in the absence of DNM (data not shown). The results obtained were similar in both parasite lines, suggesting that MDR parasites do not show cross-resistance against agarofuran sesquiterpenes. Table 1 shows that after 72 h incubation of MDR parasites in the presence of 150 μM DNM with increasing amounts of sesquiterpenes, a concentration-dependent growth inhibition (GI) was observed as compared with MDR control parasites, grown with the same DNM concentration but in the absence of a modulator.

Table 3. Experimental and CoMSIA Predicted Percent Inhibition of Grown in MDR and WT *L. tropica* Lines for Sesquiterpenes 1−30 (3 μM) and Their Solvation Free Energy (ΔG_{solv})

					MDR line		WT line		
compd	C-2	C-6	C-9	C-15	exp	pred	exp	pred	ΔG_{solv}
1	OFu	OFu	OFu	CH_3	52.9	51.6	13.8	14.3	−15.5
2	OAc	OFu	OFu	CH_3	83.5	85.1	2.3	−[a]	−13.7
3	OH	OFu	OFu	CH_3	4.9	4.9	2.3	2.3	−15.5
4	OBz	OFu	OFu	CH_3	74.8	71.8	16.5	16.1	−14.0
5	OPr	OFu	OFu	CH_3	89.1	90.8	15.9	15.7	−12.8
6	OMeBut	OFu	OFu	CH_3	87.6	87.8	21.8	21.8	−12.0
7	OAc	OFu	OFu	CH_2OAc	79.6	79.7	3.1	3.1	−17.1
8	OAc	OBz	OBz	CH_2OAc	77.5	77.6	6.9	6.9	−16.3
9	H	OFu	OFu	CH_3	66.9	67.2	14.8	14.8	−11.4
10	OAc	OAc	OAc	CH_2OAc	0.0	−	0.0	−	−22.4
11	OFu	OH	OFu	CH_3	1.5	6.2	0.0	0.0	−15.7
12	OFu	OAc	OFu	CH_3	0.0	−2.3	0.0	−0.4	−15.6
13	OAc	OH	OFu	CH_3	5.5	4.7	0.0	−0.2	−13.8
14	OAc	OAc	OFu	CH_3	6.0	6.8	0.0	−0.2	−13.8
15	OAc	OMeBut	OFu	CH_3	1.4	2.6	0.0	0.0	−11.5
16	OAc	OLau	OFu	CH_3	8.8	6.8	0.0	0.2	−11.4
17	OAc	ONap	OFu	CH_3	16.5	15.5	0.0	−0.1	−13.4
18	OAc	OPiv	OFu	CH_3	44.5	43.0	0.0	0.0	−11.2
19	OAc	OTFAc	OFu	CH_3	1.7	1.5	0.0	−0.1	−10.5
20	OAc	O4-MeO-Bz	OFu	CH_3	35.4	35.0	0.0	0.4	−13.7
21	OAc	O4-NO_2-Bz	OFu	CH_3	4.9	−	0.0	0.1	−15.7
22	OBz	OH	OFu	CH_3	11.1	7.2	0.0	0.2	−14.2
23	OBz	OAc	OFu	CH_3	4.1	5.8	0.0	0.6	−14.1
24	OBz	OMeBut	OFu	CH_3	4.1	3.0	0.0	0.1	−11.8
25	OBz	OLau	OFu	CH_3	3.0	4.9	0.0	−0.2	−11.7
26	OBz	ONap	OFu	CH_3	2.4	3.5	0.0	0.1	−13.7
27	OBz	OPiv	OFu	CH_3	11.2	12.6	0.0	0.0	−11.5
28	OBz	OTFAc	OFu	CH_3	5.9	6.2	0.0	0.1	−10.7
29	OBz	O4-MeO-Bz	OFu	CH_3	0.8	1.3	0.0	−0.3	−14.1
30	OBz	O4-NO_2-Bz	OFu	CH_3	13.5	13.6	0.0	−0.1	−16.0

[a] A dash indicates that the compound was not included in the CoMSIA model.

Table 4. Statistical Results of Percent Inhibition in MDR and WT *L. tropica* Lines in CoMSIA Models

	MDR line	WT line
$q^{2\,a}$	0.790	0.715
N[b]	19	18
n[c]	28	28
$r^{2\,d}$	0.997	0.999
F	155.752	426.658
electrostatic[e]	58.9	54.5
steric[e]	5.4	8.2
H-bond donor[e,f]	13.3	9.6
H-bond acceptor[e,f]	7.5	7.3
hydrophobicity[e]	10.0	17.1
solvation[e]	4.9	3.3

[a] Leave-one-out correlation coefficient. [b] Optimal number of principal components. [c] Number of compounds. [d] Non-cross-validated correlation coefficient. [e] Percentage of contribution. [f] On the receptor.

Scheme 1

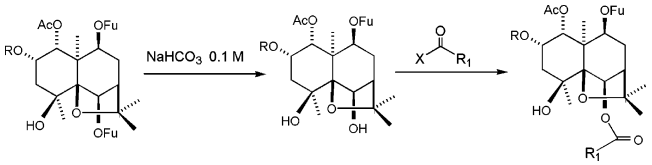

The chemosensitization to 150 μM DNM was very efficient for compounds **2** and **4**−**8**. In this form, 3 and 7 μM of these sesquiterpenes produced 75−89% GI and 90−95% GI, respectively. All compounds tested showed a low intrinsic cytotoxicity at concentrations below 15 μM. All the chemical derivatives (compounds **11**−**30**) were inactive or less active than the natural ones. To confirm the ability of sesquiterpenes to overcome the drug resistance, we determined the IC_{50} values for DNM in the MDR line using different concentrations of the most active and selective sesquiterpenes (Table 2). In fact, 15 μM of **2**, **7**, and **8** compounds reduced the resistance index (IC_{50} ratio among MDR and WT lines) from 75.5 to 2.3, 2.9, and 5.2, respectively.

DNM resistance in the MDR *L. tropica* line is related to a decreased intracellular drug accumulation, mainly due to the Pgp-like transporter overexpression.[11] To analyze if the reversal effect observed by some sesquiterpenes correlated with an increased drug accumulation, as a consequence of the Pgp inhibition, we studied by laser flow cytometry their effect on calcein (CAL) accumulation as described.[5] Flow cytometry analysis (Figure 3) demonstrated that, as expected, the MDR line accumulated a significantly lower amount of dye, expressed as mean fluorescence channel (m = 384), than the WT line (m = 582). Coincubation of the MDR parasites with 5 μM of one of the most active sesquiterpenes (compound **2**) resulted in a significant shift of the peak of fluorescence distribution to the right, almost to the WT level (m = 528); this reversal effect was a consequence of an increased CAL accumulation, probably due to Pgp-like transporter inhibition. The same concentration of sesquiterpenes that gave a moderate reversal effect only produced a slight increase of the intracellular dye (m = 382−399). Indeed, Figure 3 shows that different sesquiterpenes with distinct reversal efficiencies restored the dye accumulation in the MDR line with an order of efficiency similar to that obtained with the DNM chemosensitization experiments, **7** > **2** ≫ **14** > **3** > **13**, with no significant effects in the WT line (not shown). The effects of sesquiterpenes as reversal agents of the MDR phenotype seem not to be

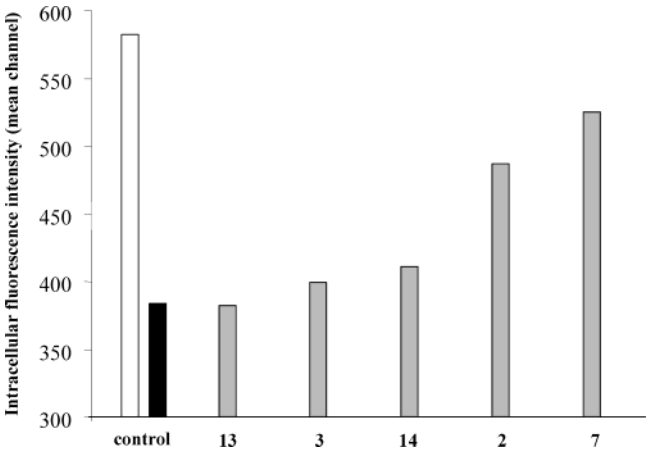

Figure 3. Differential modulation by sesquiterpenes of CAL accumulation in a MDR *L. tropica* line. Fluorescence intensity histograms were obtained by flow cytometry after incubation for 1 h at 28 °C with 2 μM of CAL-acetoxymethyl ester (CAL-AM) in the presence or absence of 5 μM sesquiterpenes. A total of 10 000 cells were counted for each histogram. Experiments were repeated three times and gave essentially the same profiles as the ones shown here. WT (white bar) and MDR (black bar) parasites were incubated with CAL-AM and used as control of CAL accumulation. MDR parasites (grey bars) incubated with CAL-AM in the presence of different sesquiterpenes (**2**, **3**, **7**, **13**, and **14**).

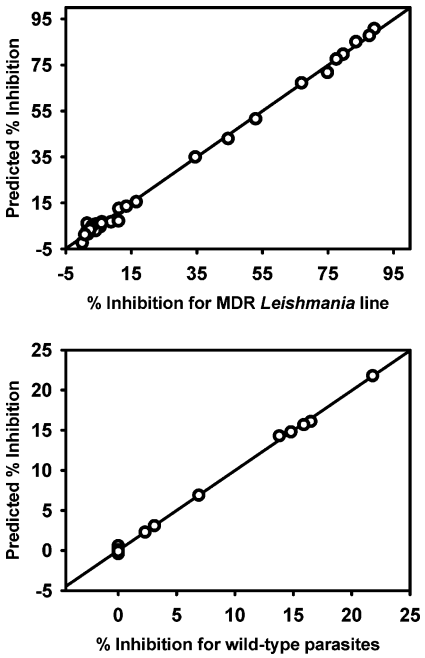

Figure 4. Plot of the predicted versus the experimental percent inhibition for the MDR and WT *L. tropica* lines by applying CoMSIA models.

related with the binding to the cytosolic nucleotide domains of Pgp-like transporter,[17] suggesting the binding to the transmembrane domains and the block of DNM efflux.

3D-QSAR/CoMSIA analysis was performed on the sesquiterpenes **1**−**30** (Table 3). Compounds **10** and **21** for the MDR line and compounds **2** and **10** for the WT line were not included in the CoMSIA model, because their residual values were greater than two standard deviations. Thus, the % GI produced by 3 μM of sesquiterpenes **1**−**9** and **11**−**30** in the MDR line and by sesquiterpenes **1**, **3**−**9**, and **11**−**30** in the WT line were related to the independent variables by the PLS methodology, to evaluate the potency and selectivity of these compounds.

Table 4 shows the statistical properties of the model. From a statistical viewpoint, the high values of the obtained cross-validated correlation coefficient q^2 (0.790 and 0.715 for MDR and WT lines, respectively) reveal that both models are useful tools for predicting the biological activity. In addition, the models yielded conventional r^2 of 0.997 (19 principal components) and 0.999 (18 principal components) for the MDR and WT lines, respectively. The theoretically predicted and experimentally determined inhibition values, for the whole set of compounds, are listed in Table 3 and plotted in Figure 4. The relative contributions in the MDR (58.9:5.4:13.3:7.5:10.0:4.9) and WT (54.5:8.2:9.6:7.3:17.1:3.3) CoMSIA models for the electrostatic, steric, hydrogen-bond-donor and -acceptor, hydrophobic, and solvation terms, respectively, are also shown in Table 4. Notably, the hydrophobic term is higher in the WT than in the MDR model, whereas the steric and the hydrogen-bond-donor contributions are higher in the MDR model. The other contributions remain similar in both models.

Figures 5 and 6 illustrate the CoMSIA electrostatic (i), steric (ii), hydrogen-bond-donor and -acceptor (iii), and hydrophobic (iv) maps for the MDR (A) and WT (B) models, using compounds **7** (Figure 5) and **29** (Figure 6) as the reference structures. The color code of the maps is as follows: (i) areas where a high electron density provided by the ligand increases or decreases GI are shown in red or blue, respectively; (ii) green and yellow areas depict zones of the space where occupancy by the ligands increases or decreases GI, respectively; (iii) areas where H-bond donors on the receptor are predicted to enhance or disfavor GI are shown in magenta and orange, respectively, whereas cyan contours show areas where H-bond-acceptor zones on the receptor are predicted to increase GI; and (iv) yellow and white areas define regions of space where hydrophobes and hydrophilic groups, respectively, are predicted to enhance GI.

The CoMSIA analysis allowed us to rationalize the observed data of GI. The H-bond donor (the second field contribution in the MDR model, 13.3%; see Table 4) map (Figures $5A_{iii}$ and $6A_{iii}$) shows three magenta areas: at the upper-left side (substitutions at C-2), on the right side (substitutions at C-6 and C-15), and at the bottom-center (substitution at C-6) of the figures. Structure−activity relationship (SAR) studies of the A-ring of the sesquiterpenes **1**−**6** and **9** suggest that a substituent at the C-2 position seems to be essential for the reversal activity in the MDR line. The introduction of the carbonyl group of the ester moiety (OFu, **1**; OAc, **2**; OBz, **4**; OPr, **5**; and OMeBut, **6**), capable of acting as a H-bond acceptor in the H-bond with the receptor, produces a 10-fold higher chemosensitization with respect to the presence at the same position of a hydroxyl group (OH, **3**) [e.g. GI(**3**) = 5 vs GI(**1**) = 53, GI(**2**) = 83, GI(**4**) = 75, GI(**5**) = 89, and GI(**6**) = 88] (Table 1). Clearly, there is a contact of this carbonyl group with the magenta area, which suggests a direct interaction with the receptor. It seems, on the basis of both the experimental data and the CoMSIA model, that the hydroxyl group of **3** or the equivalently positioned ether group of **1**, **2**, **4**, **5**, or **6** is

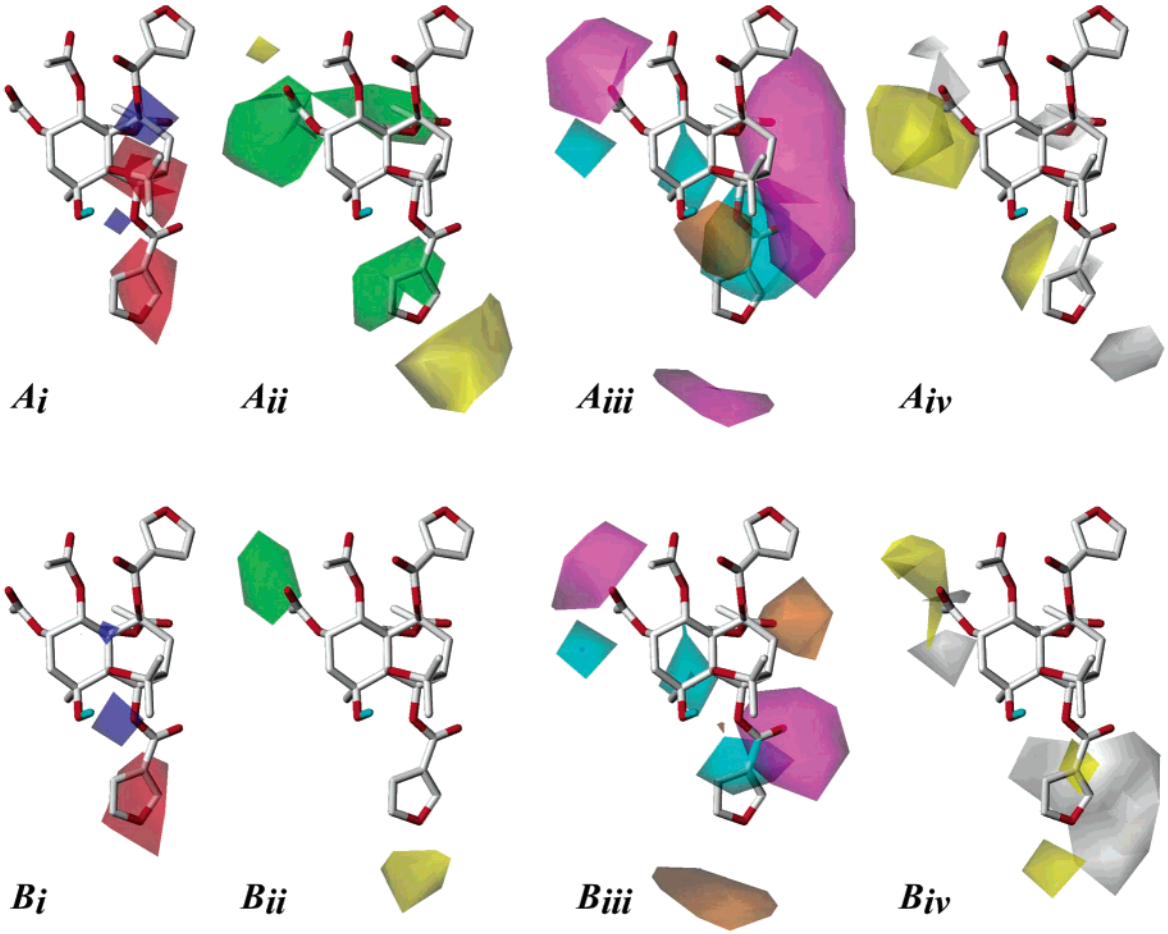

Figure 5. Electrostatic (i), steric (ii), hydrogen-bond-donor and -acceptor (iii), and hydrophobic (iv) maps for MDR (A) and WT (B) *L. tropica* lines from CoMSIA models. Compound **7** is shown as reference structure. The color code is as follows: (i) areas where a high electron density provided by the ligand increases (red) or decreases (blue) GI; (ii) green and yellow areas depict zones of the space where occupancy by the ligands increases or decreases GI, respectively; (iii) areas where H-bond donors on the receptor are predicted to enhance (magenta) or disfavor (orange) GI, whereas cyan contours show areas where H-bond acceptor zones on the receptor are predicted to increase GI; and (iv) yellow and white areas defines regions of space where hydrophobes and hydrophilic groups, respectively, are predicted to enhance GI.

not directly involved in the interaction with the receptor. Thus, removal of the hydroxyl group at the C-2 position (H, **9**) also enhances the GI for the MDR line [e.g. GI(**3**) = 5 vs GI(**9**) = 67]. The lack of interaction of the hydroxyl group with this domain of the receptor does not compensate for the energy cost of desolvating the HO-substituted ligand [ΔG_{solv}(**3**) = −15.5 kcal/mol vs ΔG_{solv}(**9**) = −11.4 kcal/mol; see Table 3]. Moreover, the hydrophobicity map (the third field contribution in the MDR model, 10.0%) displays both a yellow and a small white area at this C-2 position (Figures 5A$_{iv}$ and 6A$_{iv}$). Thus, the hydrophobic and bulky groups Bz, Pr, and MeBut of the OBz (**4**), OPr (**5**), and OMeBut (**6**) substituents, respectively, elicit some of the highest values of GI in the MDR line (Table 3). It is important to note that the Bz group has the lowest value of GI among these substituents. This finding explains the presence of the white area (regions where hydrophilic groups enhance GI or hydrophobic groups diminishes GI) at the upper-left part of the map, since the hydrogens of the Bz moiety of the OBz substituent reach this white area (Figure 6A$_{iv}$). The steric map (the fifth field contribution in the MDR model, 5.4%) reinforces this findings. Thus, OPr (**5**) and OMeBut (**6**) substituents at the C-2 position occupy the favorable green area (Figure 5A$_{ii}$) increasing GI in the MDR line, whereas the OBz (**4**) reaches the unfavorable yellow (Figure 6A$_{ii}$) zone leading to lower value than expected (Table 3).

The OFu substituent at C-6 in compounds **1**, **2**, and **4** was replaced by a hydroxyl (**11**, **13** and **22**) or an ester (**12**, **14**−**21**, **23**−**30**) group. Comparison of their activities shows that the substituent at the C-6 position is crucial for the modulation of the activity. The presence of a hydroxyl (**11**, **13** and **22**) or acetate (**12**, **14** and **23**) group at the 6-position has a detrimental effect on GI with respect to the presence of a furoate group (**1**, **2**, and **4**) [e.g. GI(**1**) = 53 vs GI(**11**) = 1, GI(**12**) = 0; GI(**2**) = 84 vs GI(**13**) = 5, GI(**14**) = 6; and GI(**4**) = 75 vs GI(**22**) = 11, GI(**23**) = 4] (Table 1). Thus, the oxygen of the furan ring of the OFu substituent seems to act as a H-bond acceptor in the interaction with the receptor (see magenta area at the bottom side of Figure 5A$_{iii}$). Accordingly, the electrostatic map (the highest field contribution in the MDR model, 58.9%) shows a red area (Figure 5A$_{i}$) at this position of the furan ring, emphasizing the importance of this part of the molecule in the interaction with the receptor. While the energy cost of desolvating the hydroxyl or the acetate substituent is similar to that of the corresponding furoate [ΔG_{solv}(**1**) = −15.5 vs ΔG_{solv}(**11**) = −15.7, ΔG_{solv}(**12**) = −15.6;

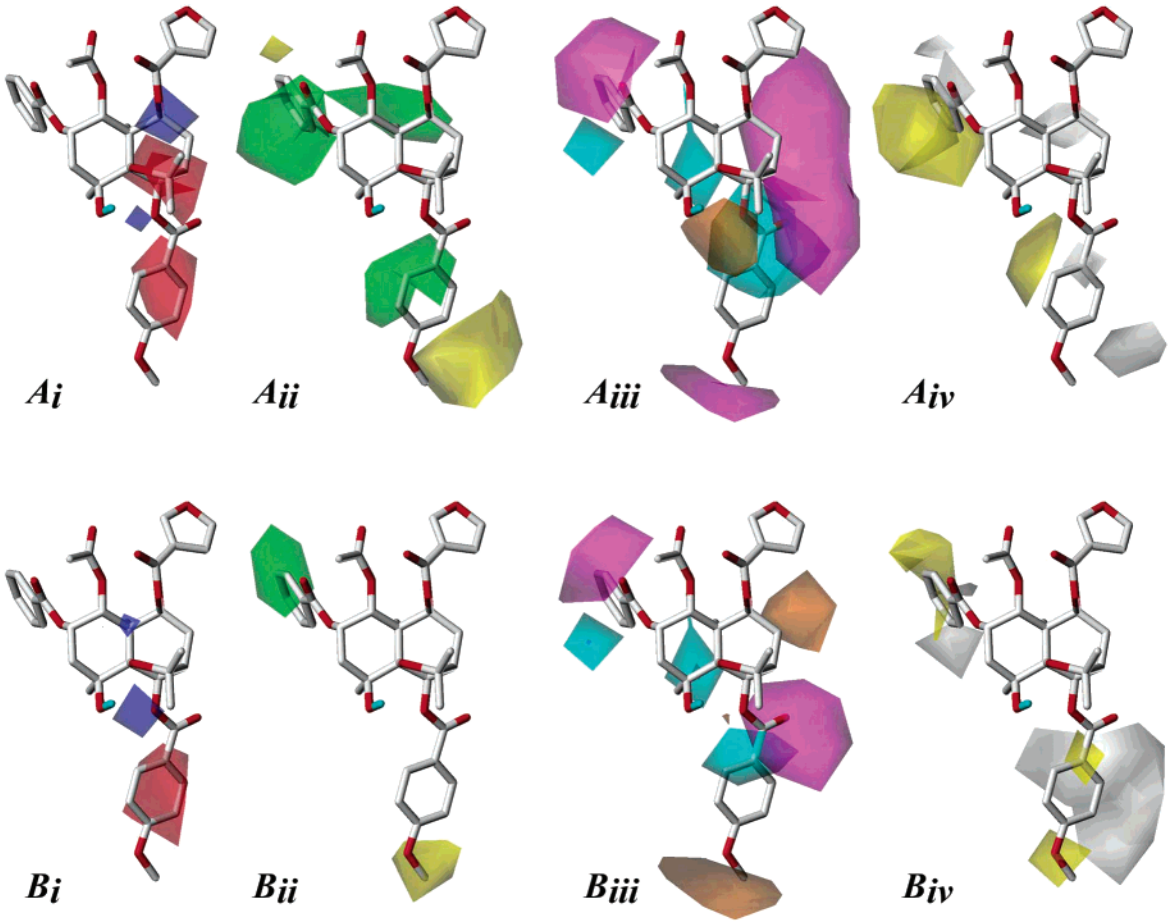

Figure 6. Electrostatic (i), steric (ii), hydrogen-bond-donor and -acceptor (iii), and hydrophobic (iv) maps for MDR (A) and WT (B) *L. tropica* lines from CoMSIA models. Compound **29** is shown as reference structure. The color code is the same as in Figure 5.

ΔG_{solv}(**2**) = −13.7 vs ΔG_{solv}(**13**) = −13.8, ΔG_{solv}(**14**) = −13.8; and ΔG_{solv}(**4**) = −14.0 vs ΔG_{solv}(**22**) = −14.2, ΔG_{solv}(**23**) = −14.1], their shortest side chain impedes the interaction with this part of the receptor, leading to lower values of GI. Additionally, the hydrophobicity map (Figure 5A$_{iv}$) also displays a yellow area in the vicinity of this furan ring. Thus, it seems reasonable to propose that the electron-poor C−H hydrogens of the furan ring also interact with the receptor.[32] Consequently, the steric map (Figure 5A$_{ii}$) shows at the C-6 position a favorable green area near these furan hydrogens. Notably, the OPiv (**18**) substituent (derived from compound **2** that contains the optimal OAc substituent at the C-2 position) lacks the polar oxygen of the furan ring but contains electron-poor C−H hydrogens, thus possessing intermediate GI values [GI(**2**) = 84 vs GI(**18**) = 45]. Longer and hydrophobic side chains (**15**−**17**) would occupy the yellow (disfavorable) area in the steric map, whereas the longer and polar O4−NO_2−Bz side chain (**21**) requires higher solvation energy (see Table 3), which is not compensated by the interaction with the receptor, leading to low values of GI. The intermediate values of GI of compound **20** (GI = 35) led us to suggest that the OCH_3 moiety of the O4−MeO−Bz substituent is able to H-bond the receptor as the oxygen atom of the furan ring, but its longer side chain occupies the yellow (disfavorable) area in the steric map (Figure 6A$_{ii}$).

On the other hand, the regiosubstitution seems to be an important element for affinity, since the tetrasubstituted 4β-hydroxydihydro-β-agarofuran sesquiterpenes **2** and **12** have the same molecular formula, the only difference being the presence of the acetate or furoate at the C-2 and C-6 positions. Compound **2** has OAc at C-2 and OFu at C-6, contrarily to **12**, because **12** is completely inactive and **2** shows strong activity [e.g. GI(**2**) = 83 vs GI(**12**) = 0].

Moreover, compounds **2** (CH_3) and **7** (CH_2OAc) led us to study the effect of the substituent at the C-15 position in GI. The addition of the polar OAc moiety does not affect GI [GI(**2**) = 83 vs GI (**7**) = 80]. However, the energy cost of desolvating the CH_2OAc-substituted ligand [ΔG_{solv}(**7**) = −17.1 kcal/mol] is higher than for the CH_3-substituted ligand [ΔG_{solv} (**2**) = −13.7 kcal/mol]. Thus, this additional energy penalty of **7** relative to **2** due to solvation must be compensated by additional interactions of **7** with the receptor. Accordingly, Figures 5 and 6 depict a magenta H-bond-donor area and a favorable green area (steric map) on this part of the receptor that enhances GI.

Finally, the OH substituent at the C-4 position of these sesquiterpenes is located close to the orange contours (Figure 5A$_{iii}$). This orange region predicts the position where an H-bond donor zone/residue in the receptor probably disfavors binding. On the other hand, the OAc and the OFu/OBz substituents at the C-1 and C-9 positions, respectively, are located close to the

magenta area (Figure 5A$_{iii}$). Thus, these groups may form hydrogen bonds with H-bond donor zones/residues in the receptor. However, the absence of variability at any of these positions in the studied series of compounds prevents reaching any further conclusion.

Compounds **1**−**2**, **4**−**6**, and **9** produced limited effects on the WT parasites, which could correspond to some low binding to other cellular targets. The presence of an acetate (**2**), protons (**9**), furoate (**1**), propianate (**5**), benzoate (**4**), or methylbutyrate (**6**) at C-2 increases the cytotoxic effects of these compounds in the rank order of **2** < **1** < **9** < **5** < **4** < **6**. These compounds produced in the WT line a 2%, 14%, 15%, 16%, 17%, or 22% inhibition of growth, respectively. These studies allowed us to establish that the acetate group is the optimal structural feature at C-2, in terms of both potency and selectivity for the MDR line; thus, compound **2** represents the most active member of these sesquiterpenes (**1**−**6** and **9**). The B panels in Figures 5 and 6 illustrate the CoMSIA maps for the WT line. The substituent at the C-2 position also seems important for GI in the WT line as shown in the steric (B$_{ii}$), H-bond-donor and -acceptor (B$_{iii}$), and hydrophobic (B$_{iv}$) maps. The effect on GI of the different substituents at this position of the molecule followed the same trend as for the MDR line (see above) with the exception of compound **2** (OAc). The CH_3 moiety of the OAc substituent in C-2 does not contact the favorable green region in the steric map (Figure 5B$_{ii}$). Thus, the bulky substituents of compounds **1** (OFu), **4** (OBz), **5** (OPr), and **6** (OMeBut) and the unsubstituted compound **9** (H) have larger values of GI than compounds **2** (OAc) and **3** (OH). The steric interactions of the bulky substituents (OFu, **1**; OAc, **2**; OBz, **4**; OPr, **5**; and OMeBut, **6**) with the receptor (Figures 5 and 6, panel B$_{ii}$) or the facility of desolvating compound **9** are responsible for high values of GI.

However, the most important position for GI in the WT line is C-6. Substitution of the polar OFu group (**1**−**7**, **9**), involved in electrostatic interaction [the highest field contribution in the WT model is 54.5% (see the red contour at the bottom-center part of Figure 5B$_i$)], with other groups in **11**−**30** [by OH (**11** and **13**), OAc (**12** and **14**), OMeBut (**15** and **24**), OLau (**16** and **25**), ONap (**17** and **26**), OPiv (**18** and **27**), OTFAc (**19** and **28**), O4-MeO−Bz (**20** and **29**), or O4−NO_2−Bz (**21** and **30**)] leads to compounds with the desirable lack of activity in WT (GI values of 0, Table 3). It seems that precisely the absence of the negative charge generated by the oxygen of the OFu substituent impedes compounds **11**−**30** from interacting with the receptor at this position (panels B in Figure 6).

This is corroborated by the orange region (area of the receptor where H-bond donors disfavor GI, panels B$_{iii}$ in Figures 5 and 6) at this position in the WT line that contrast with the magenta region (area of the receptor where H-bond donors enhance GI, panels A$_{iii}$ in Figures 5 and 6) in the MDR line.

Another significant difference between the WT and MDR maps resides in the H-bond-donor/acceptor map at the C-15 position. While the map for the MDR line also contains a magenta area at this position, the map for the WT line contains an orange area (Figures 5 and 6, parts A$_{iii}$ and B$_{iii}$).

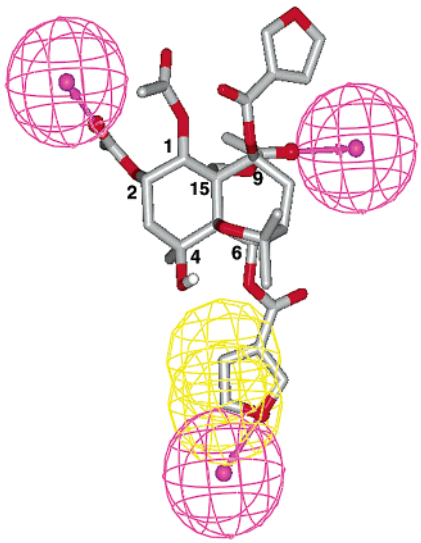

Figure 7. Most salient structural elements of the ligands that are key to high growth inhibition obtained with the 3D-QSAR/CoMSIA methodology. Magenta spheres represent areas of the receptor that interact with H-bond-acceptor moieties of the ligand (i.e. the carbonyl group at the C-2 position and the oxygen of the furan ring at the C-6 position). Yellow spheres represent areas of the receptor that interact with hydrophobic moieties of the ligand (i.e. the C−H groups of the furan ring at the C-6 position).

Macrocyclic compound **10** showed no activity due to its too bulky cycle that might not fit into the active site. These results are in agreement with previous observations that the steric properties could modulate the activity.[5]

Conclusions

3D-QSAR/CoMSIA methodology has been successfully applied to explain the reversal activity of a series of sesquiterpenes **1**−**30** against the MDR phenotype of *Leishmania*. The derived computational model has facilitated the identification of the structural elements of the ligands, depicted in Figure 7, that are key to high growth inhibition. The most salient features of the electrostatic, steric, hydrogen-bond-donor and -acceptor, and hydrophobic maps obtained with the 3D-QSAR/CoMSIA methodology are the following. The carbonyl group of the OFu (**1**), OAc (**2**), OBz (**4**), OPr (**5**), and OMeBut (**6**) substituents at the C-2 position acts as a H-bond acceptor in the H-bond with an area of the receptor depicted as a magenta sphere (Figure 7). The oxygen of the furan ring at the C-6 position seems to form a hydrogen bond with the receptor (see magenta sphere in Figure 7). The C−H moieties of the furan ring at the C-6 position are also involved in the interaction with the receptor (yellow sphere). Moreover, the CH_2-OAc group at the C-15 position in compound **7** is engaged in the H-bond interaction with an area of the receptor depicted as a magenta sphere (Figure 7). The substituents at the C-1, C-4, and C-9 positions of sesquiterpenes may also be engaged in H-bond interactions with the receptor. However, the absence of variability at any of these positions in the studied series of compounds impedes any further conclusion. Finally, replacement of the furoate group by a benzoate group at both C-6 and C-9 does not modify GI but slightly increases the cytotoxic effect. These results support the

importance of both hydrogen-bond donors and acceptors in inhibitor binding to a Pgp-like transporter.

Sesquiterpenes **2**, **7**, and **8** showed a high reversal activity on the DNM-resistant phenotype in *Leishmania* with values of GI at 3 μM higher than 75% and very low values of intrinsic toxicities, being, at present, the most effective agarofuran sesquiterpenes tested. These results together with other obtained in previous works[5,6,17] will be used to design and synthesize more effective and specific new Pgp-like inhibitors. Moreover, further studies are in progress to increase our knowledge about the mode of action of these compounds.

Experimental Section

General Experimental Procedures. Optical rotations were measured on a Perkin-Elmer 241 automatic polarimeter, and the $[\alpha]_D$ are given in 10^{-1} deg cm^2 g^{-1}. IR (film) spectra were recorded on a Bruker IFS 55 spectrophotometer. ^{1}H NMR spectra were recorded on a Bruker Avance 400 or a Bruker Avance 300 spectrometer. EIMS and HREIMS were recorded on a Micromass Autospec spectrometer. Monitoring and purification of the reactions were performed using silica gel (TLC, plastic sheets, silica gel 60−250 UV_{250}, Panreac). All reagents were purchased from Aldrich and used without further purification.

Chemistry. 1α-Acetoxy-2α,9*β*-difuroyloxy-4*β*,6*β*-dihydroxydihydro-*β*-agarofuran (11). A mixture of **1** (10.0 mg), methanol (3 mL), acetone (2 mL), and $NaHCO_3$ (1 mL, 0.1 M) was refluxed for 5 h. Then the mixture was concentrated under reduced pressure, water was added to the residue, and the aqueous residue was extracted three times with ethyl acetate. The collected organic layers were dried over magnesium sulfate and evaporated under reduced pressure to give a thick oil, which was purified by preparative TLC using *n*-hexane/ethyl acetate (1/1) to give **11** (8.2 mg): colorless lacquer; $[\alpha]^{25}_D = +39.4°$ (*c* 0.34, $CHCl_3$); IR γ_{max} (film) 3433, 2925, 2853, 1746, 1720, 1312, 1244, 1162, 1140, 763 cm^{-1}; ^{1}H NMR ($CDCl_3$) δ 1.52 (6H, s), 1.60 (3H, s), 1.71 (3H, s), 1.83 (3H, s), 2.16 (5H, m), 3.31 (1H, s), 4.56 (1H, s), 4.87 (1H, d, J = 6.9 Hz), 4.97 (1H, s), 5.49 (1H, d, J = 3.7 Hz), 5.73 (1H, m), 6.70 (1H, s), 6.73 (1H, s), 7.42 (1H, d, J = 1.5 Hz), 7.45 (1H, d, J = 1.5 Hz), 7.97 (1H, d, J = 0.7 Hz), 8.01 (1H, d, J = 0.7 Hz); MS (EI) *m*/*z* (%) 532 (M$^+$, 1), 517 (4), 420 (3), 405 (11), 345 (1), 233 (4), 205 (4), 168 (6), 149 (16), 95 (100); HRMS (EI) *m*/*z* calcd for $C_{27}H_{32}O_{11}$ 532.19446, found 532.19138.

1α,6*β*-Diacetoxy-2α,9*β*-difuroyloxy-4*β*-hydroxydihydro-*β*-agarofuran (12). A mixture of acetic anhydride (4 drops), compound **11** (4.0 mg), and 4-(dimethylamino)pyridine (2.0 mg) in pyridine (2 drops) was stirred at room temperature for 16 h. The mixture was evaporated to dryness, and the residue was purified by preparative TLC using *n*-hexane/ethyl acetate (3/2) to give **12** (3.5 mg): colorless lacquer; $[\alpha]^{25}_D = +30.0°$ (*c* 0.10, $CHCl_3$); IR γ_{max} (film) 3446, 2925, 2853, 1731, 1368, 1309, 1260, 1160, 1024, 799 cm^{-1}; ^{1}H NMR ($CDCl_3$) δ 1.50 (3H, s), 1.56 (3H, s), 1.59 (6H, s), 1.73 (3H, s), 2.14 (3H, s), 2.10−2.19 (4H, m), 2.47 (1H, m), 3.59 (1H, s), 4.91 (1H, d, J = 6.7 Hz), 5.46 (1H, d, J = 3.5 Hz), 5.61 (1H, s), 5.69 (1H, m), 6.69 (1H, d, J = 1.3 Hz), 6.73 (1H, d, J = 1.3 Hz), 7.42 (1H, d, J = 1.7 Hz), 7.44 (1H, d, J = 1.7 Hz), 7.95 (1H, s), 8.03 (1H, s); MS (EI) *m*/*z* (%) 574 (M$^+$, 1), 559 (2), 514 (1), 447(5), 402 (14), 290 (8), 192 (10), 95 (100); HRMS (EI) *m*/*z* calcd for $C_{29}H_{34}O_{12}$ 574.20502, found 574.20781.

1α,2α-Diacetoxy-9*β*-furoyloxy-4*β*,6*β*-dihydroxydihydro-*β*-agarofuran (13). Compound **2** (120.0 mg) was treated under the conditions already described for the synthesis of **11**, affording **13** (114.1 mg): colorless lacquer; $[\alpha]^{25}_D = +12.8°$ (*c* 0.25, $CHCl_3$); IR γ_{max} (film) 3536, 2959, 1746, 1721, 1366, 1244, 1140, 1026, 762 cm^{-1}; ^{1}H NMR ($CDCl_3$) δ 1.46 (3H, s), 1.51 (3H, s), 1.58 (3H, s), 1.70 (3H, s), 1.78 (3H, s), 2.06 (3H, s), 2.00−2.32 (5H, m), 3.27 (1H, s), 4.53 (1H, d, J = 5.3 Hz), 4.85 (1H, d, J = 6.7 Hz), 4.96 (1H, d, J = 5.3 Hz), 5.41 (1H, d, J = 3.6 Hz), 5.54 (1H, m), 6.72 (1H, t, J = 0.7 Hz), 7.41 (1H, s), 8.00 (1H, d, J = 0.7 Hz); MS (EI) *m*/*z* (%) 480 (M$^+$, 3), 465 (25), 420 (10), 353 (35), 233 (13), 168 (12), 95 (100); HRMS (EI) *m*/*z* calcd for $C_{24}H_{32}O_{10}$ 480.19955, found 480.20226.

1α,2α,6*β*-Triacetoxy-9*β*-furoyloxy-4*β*-hydroxydihydro-*β*-agarofuran (14). Compound **13** (3.7 mg) was treated under the conditions already described for the synthesis of **12**, affording **14** (3.7 mg): colorless lacquer; $[\alpha]^{25}_D = +7.6°$ (*c* 0.34, $CHCl_3$); IR γ_{max} (film) 3547, 2927, 2855, 1747, 1720, 1367, 1309, 1243, 1160, 762 cm^{-1}; ^{1}H NMR ($CDCl_3$) δ 1.49 (3H, s), 1.50 (6H, s), 1.54 (3H, s), 1.74 (3H, s), 2.05 (3H, s), 2.14 (3H, s), 1.98−2.18 (4H, m), 2.47 (1H, m), 2.94 (1H, s), 4.89 (1H, d, J = 6.7 Hz), 5.39 (1H, d, J = 3.5 Hz), 5.50 (1H, m), 5.57 (1H, s), 6.73 (1H, t, J = 0.7 Hz), 7.42 (1H, t, J = 0.7 Hz), 8.01 (1H, t, J = 0.7 Hz); MS (EI) *m*/*z* (%) 522 (M$^+$, 1), 507 (2), 480 (3), 462 (4), 420 (4), 402 (19), 233 (9), 192 (17), 95 (50), 57 (100); HRMS (EI) *m*/*z* calcd for $C_{26}H_{34}O_{11}$ 522.21011, found 522.20712.

1α,2α-Diacetoxy-9*β*-furoyloxy-6*β*-(*S*)-(+)-2-methylbutyroyloxy-4*β*-hydroxydihydro-*β*-agarofuran (15). A mixture of (*S*)-(+)-2-methylbutyric anhydride (6 drops), triethylamine (10 drops), compound **13** (4.0 mg), and 4-(dimethylamino)-pyridine (2.0 mg) in dry dichloromethane (1 mL) was refluxed for 16 h. The mixture was evaporated to dryness, and the residue was purified by preparative TLC using *n*-hexane/ethyl acetate (3/2) to give **15** (3.2 mg): colorless lacquer $[\alpha]^{20}_D = +5.0°$ (*c* 0.24, $CHCl_3$); IR γ_{max} (film) 3547, 2962, 2928, 1745, 1731, 1366, 1243, 1147, 1070, 1027, 762 cm^{-1}; ^{1}H NMR ($CDCl_3$) δ 0.91 (3H, t, J = 7.5 Hz), 1.19 (3H, d, J = 7.0 Hz), 1.46 (1H, m), 1.50 (3H, s), 1.51 (3H, s), 1.55 (3H, s), 1.56 (3H, s), 1.73 (3H, s), 1.74 (1H, m), 2.05 (3H, s), 1.94−2.20 (4H, m), 2.50 (2H, m), 2.92 (1H, s), 4.90 (1H, d, J = 6.8 Hz), 5.39 (1H, d, J = 3.5 Hz), 5.50 (1H, m), 5.62 (1H, s), 6.73 (1H, d, J = 1.6 Hz), 7.41 (1H, d, J = 1.6 Hz), 8.01 (1H, s); MS (EI) *m*/*z* (%) 549 (M$^+$ − 15, 4), 504 (1), 480 (5), 462 (1), 437 (15), 402 (32), 290 (18), 233 (14), 192 (23), 95 (74), 57 (100); HRMS (EI) *m*/*z* calcd for $C_{28}H_{37}O_{11}$ 549.23359, found 549.23331.

1α,2α-Diacetoxy-9*β*-furoyloxy-6*β*-lauroyloxy-4*β*-hydroxydihydro-*β*-agarofuran (16). Lauroyl chloride (0.1 mL) was added to a solution of **13** (4.0 mg), triethylamine (0.4 mL), and 4-(dimethylamino)pyridine (2.0 mg) in dry dichloromethane (1 mL) at 0 °C. The resulting mixture was stirred for 2 h at room temperature. The reaction was quenched by the addition of ethanol (0.5 mL) followed by stirring for 30 min. The mixture was evaporated to dryness, the residue was purified by flash column chromatography on silica gel (eluting 50% to 100% ethyl ether in *n*-hexane), and finally the compound was purified by preparative TLC using dichloromethane/ethyl ether (5/1) to give **16** (2.3 mg): colorless lacquer; $[\alpha]^{20}_D = +8.3°$ (*c* 0.18, $CHCl_3$); IR γ_{max} (film) 3554, 2924, 2853, 1747, 1366, 1310, 1243, 1158, 762 cm^{-1}; ^{1}H NMR ($CDCl_3$) δ 0.88 (3H, t, J = 5.5 Hz), 1.25 (14H, s), 1.50 (3H, s), 1.57 (3H, s), 1.63 (6H, s), 1.57−1.65 (4H, m), 1.74 (3H, s), 2.04 (3H, s), 1.94−2.17 (4H, m), 2.37 (2H, dt, J = 2.4, 7.3 Hz), 2.46 (1H, m), 2.92 (1H, s), 4.89 (1H, d, J = 6.6 Hz), 5.38 (1H, d, J = 3.4 Hz), 5.50 (1H, m), 5.59 (1H, s), 6.72 (1H, d, J = 1.1 Hz), 7.41 (1H, d, J = 1.1 Hz), 8.01 (1H, s); MS (EI) *m*/*z* (%) 647 (M$^+$ − 15, 9), 602 (2), 535 (11), 480 (14), 463 (3), 420 (9), 402 (67), 192 (34), 126(47), 95 (100); HRMS (EI) *m*/*z* calcd for $C_{35}H_{51}O_{11}$ 647.34314, found 647.34390.

1α,2α-Diacetoxy-9*β*-furoyloxy-6*β*-(1)-naphthoyloxy-4*β*-hydroxydihydro-*β*-agarofuran (17). A solution of **13** (3.0 mg), 1-naphthoyl chloride (0.1 mL), 4-(dimethylamino)pyridine (1.0 mg), and triethylamine (0.4 mL) in dry dichloromethane (1 mL) was refluxed for 2 h. The reaction was quenched by the addition of ethanol (0.5 mL) followed by stirring for 30 min at room temperature. The mixture was evaporated to dryness, the residue was purified by flash column chromatography on silica gel (eluting 50% to 100% dichloromethane in *n*-hexane), and finally the compound was purified by preparative TLC using *n*-hexane/ethyl acetate (3/2) to give **17** (3.0 mg): colorless lacquer; $[\alpha]^{20}_D = +23.9°$ (*c* 0.28, $CHCl_3$); IR γ_{max} (film) 3546, 2924, 2853, 1747, 1716, 1366, 1244, 1134, 787, 761 cm^{-1}; ^{1}H NMR ($CDCl_3$) δ 1.53 (3H, s), 1.56 (6H, s), 1.60 (3H,s), 1.76 (3H, s), 2.05 (1H, m), 2.07 (3H, s), 2.22 (2H, m), 2.40 (1H, s), 2.64 (1H, m), 3.19 (1H, s), 4.98 (1H, d, J = 6.8 Hz), 5.46 (1H, d, J = 3.4 Hz), 5.55 (1H, m), 5.93 (1H, s), 6.75 (1H, d, J = 1.1 Hz),

7.43 (1H, d, J = 1.1 Hz), 7.56 (2H, m), 7.65 (1H,m), 7.91 (1H, d, J = 8.2 Hz), 8.03 (1H, s), 8.07 (1H, d, J = 8.5 Hz), 8.71 (1H, d, J = 7.4 Hz), 9.20 (1H, d, J = 8.6 Hz); MS (EI) m/z (%) 634 (M^+, 1), 619 (1), 574 (1), 507 (2), 462 (1), 402 (9), 290 (2), 192 (2), 155 (100), 127 (8), 95 (9); HRMS (EI) m/z calcd for $C_{35}H_{38}O_{11}$ 634.24141, found 634.24117.

1α,2α-Diacetoxy-9β-furoyloxy-6β-pivaloyloxy-4β-hydroxydihydro-β-agarofuran (18). A solution of **13** (4.0 mg), pivaloyl chloride (0.1 mL), 4-(dimethylamino)pyridine (1.5 mg), and pyridine (0.4 mL) in dry chloroform (1 mL) was refluxed for 16 h. The reaction was quenched by the addition of ethanol (0.5 mL) followed by stirring for 30 min at room temperature. The mixture was evaporated to dryness, the residue was purified by flash column chromatography on silica gel (eluting 50% to 100% dichloromethane in *n*-hexane), and finally the compound was purified by preparative TLC using *n*-hexane/ethyl acetate (3/2) to give **18** (3.5 mg): colorless lacquer; $[\alpha]^{20}_D$ = +10.6° (c 0.34, $CHCl_3$); IR γ_{max} (film) 3553, 2958, 2925, 2853, 1748, 1721, 1366, 1244, 1148, 1070, 1027, 762 cm^{-1}; ^1H NMR ($CDCl_3$) δ 1.24 (9H, s), 1.49 (6H, s), 1.50 (3H, s), 1.55 (3H, s), 1.73 (3H, s), 2.04 (3H, s), 1.94−2.19 (4H, m), 2.46 (1H, m), 2.90 (1H, s), 4.90 (1H, d, J = 6.8 Hz), 5.40 (1H, d, J = 3.5 Hz), 5.50 (1H, m), 5.62 (1H, s), 6.72 (1H, d, J = 1.1 Hz), 7.41 (1H, t, J = 1.1 Hz), 8.01 (1H, s); MS (EI) m/z (%) 549 (M^+ − 15, 6), 437 (15), 402 (52), 290 (20), 233 (16), 192 (40), 173 (12), 149 (23), 57 (100); HRMS (EI) m/z calcd for $C_{28}H_{37}O_{11}$ 549.23359, found 549.23498.

1α,2α-Diacetoxy-9β-furoyloxy-6β-trifluoroacetoxy-4β-hydroxydihydro-β-agarofuran (19). Trifluoroacetic anhydride (3 drops) was added to a solution of **13** (3.0 mg) and pyridine (4 drops) in dry dichloromethane (1 mL) at 0 °C. After 5 min of stirring the mixture was evaporated to dryness, and the residue was purified by preparative TLC using *n*-hexane/ethyl acetate (3/2) to give **19** (2.4 mg): colorless lacquer; $[\alpha]^{20}_D$ = +13.6° (c 0.22, $CHCl_3$); IR γ_{max} (film) 3449, 2925, 2854, 1775, 1750, 1369, 1221, 1174, 1142, 1038, 762 cm^{-1}; ^1H NMR ($CDCl_3$) δ 1.48 (3H, s), 1.51 (3H, s), 1.57 (3H, s), 1.73 (3H, s), 1.94 (3H, s), 2.07 (3H, s), 2.22−2.54 (4H, m), 3.12 (1H, dd, J = 3.4, 14.7 Hz), 4.94 (1H, d, J = 6.7 Hz), 5.51 (1H, d, J = 3.6 Hz), 5.63 (1H, m), 5.68 (1H, s), 6.72 (1H, d, J = 1.7 Hz), 7.42 (1H, d, J = 1.7 Hz), 8.02 (1H, s); MS (EI) m/z (%) 558 (M^+ − 18, 1), 543 (1), 503 (1), 449 (8), 405 (0.9), 329 (1), 290 (1), 247 (2), 230 (2), 215 (2), 149 (9), 95 (100); HRMS (EI) m/z calcd for $C_{26}H_{29}O_{10}F_3$ 558.17128, found 558.17567.

1α,2α-Diacetoxy-9β-furoyloxy-6β-(4)-methoxybenzoyloxy-4β-hydroxydihydro-β-agarofuran (20). Compound **13** (3.0 mg) was treated with 4-methoxybenzoyl chloride (0.1 mL) under the conditions already described for the synthesis of **18**, affording **20** (2.7 mg): colorless lacquer; $[\alpha]^{20}_D$ = +14.5° (c 0.22, $CHCl_3$); IR γ_{max} (film) 3547, 2924, 2852, 1746, 1717, 1606, 1366, 1312, 1254, 1163, 1027, 761 cm^{-1}; ^1H NMR ($CDCl_3$) δ 1.51 (3H, s), 1.53 (3H, s), 1.54 (3H, s), 1.56 (3H, s), 1.75 (3H, s), 2.04 (3H, s), 1.99−2.24 (3H, m), 2.36 (1H, m), 2.56 (1H, m), 3.13 (1H, s), 3.87 (3H, s), 4.94 (1H, d, J = 6.7 Hz), 5.43 (1H, d, J = 3.4 Hz), 5.53 (1H, m), 5.70 (1H, s), 6.74 (1H, t, J = 1.1 Hz), 6.96 (2H, dd, J = 2.7, 8.9 Hz), 7.42 (1H, t, J = 1.7 Hz), 8.03 (1H, t, J = 0.7 Hz), 8.15 (2H, dd, J = 2.7, 8.9 Hz); MS (EI) m/z (%) 614 (M^+, 1), 599 (1), 533 (3), 502 (10), 402 (39), 290 (14), 192 (47), 149 (82), 120 (97), 95 (100); HRMS (EI) m/z calcd for $C_{32}H_{38}O_{12}$ 614.23633, found 614.23883.

1α,2α-Diacetoxy-9β-furoyloxy-6β-(4)-nitrobenzoyloxy-4β-hydroxydihydro-β-agarofuran (21). Compound **13** (3.0 mg) was treated with 4-nitrobenzoyl chloride (0.1 mL) under the conditions already described for the synthesis of **18**, affording **21** (2.8 mg)**:** colorless lacquer; $[\alpha]^{20}_D$ = +22.3° (c 0.13, $CHCl_3$); IR γ_{max} (film) 3546, 2924, 2853, 1746, 1724, 1530, 1366, 1282, 1254, 1119, 1027, 760, 721 cm^{-1}; ^1H NMR ($CDCl_3$) δ 1.52 (3H, s), 1.55 (3H, s), 1.56 (6H, s), 1.75 (3H, s), 2.04 (3H, s), 2.00−2.27 (3H, m), 2.39 (1H, m), 2.57 (1H, m), 3.09 (1H, s), 4.95 (1H, d, J = 6.7 Hz), 5.43 (1H, d, J = 3.5 Hz), 5.53 (1H, m), 5.74 (1H, s), 6.74 (1H, d, J = 1.6 Hz), 7.42 (1H, t, J = 1.6 Hz), 8.03 (1H, s), 8.32 (2H, dd, J = 1.9, 6.9 Hz), 8.41 (1H, dd, J = 1.9, 6.9 Hz); MS (EI) m/z (%) 614 (M^+ − 15, 1), 590 (7), 569 (12), 502 (12), 402 (40), 290 (15), 233 (16), 192 (49), 150 (72), 120 (70), 95 (100); HRMS (EI) m/z calcd for $C_{30}H_{32}N_1O_{13}$ 614.18737, found 614.18866.

1α-Acetoxy-2α-benzoyloxy-9β-furoyloxy-4β,6β-dihydroxydihydro-β-agarofuran (22). Compound **4** (104.0 mg) was treated under the conditions already described for the synthesis of **11**, affording **22** (88.0 mg): colorless lacquer; $[\alpha]^{25}_D$ = +60° (c 0.36, $CHCl_3$); IR γ_{max} (film) 3433, 2928, 1720, 1366, 1277, 1233, 1105, 1025, 761, 711 cm^{-1}; ^1H NMR ($CDCl_3$) δ 1.53 (3H, s), 1.58 (3H, s), 1.60 (3H, s), 1.70 (3H, s), 1.86 (3H, s), 2.08−2.35 (5H, m), 3.33 (1H, s), 4.58 (1H, d, J = 5.4 Hz), 4.88 (1H, d, J = 6.7 Hz), 4.99 (1H, d, J = 5.4 Hz), 5.53 (1H, d, J = 4.0 Hz), 5.81 (1H, m), 6.73 (1H, d, J = 1.6 Hz,), 7.43 (2H, m), 7.50 (1H, d, J = 1.6 Hz), 7.59 (1H, m), 7.98 (1H, d, J = 7.4 Hz), 8.02 (1H, s); MS (EI) m/z (%) 527 (M^+ − 15, 6), 420 (5), 415 (11), 360 (1), 349 (3), 308 (3), 289 (3), 105 (100), 94 (63), 77 (21), 57 (26); HRMS (EI) m/z calcd for $C_{28}H_{31}O_{10}$ 527.19172, found 527.18518.

1α,6β-Diacetoxy-2α-benzoyloxy-9β-furoyloxy-4β-hydroxydihydro-β-agarofuran (23). Compound **22** (3.0 mg) was treated under the conditions already described for the synthesis of **12**, affording **23** (2.1 mg): colorless lacquer; $[\alpha]^{20}_D$ = +30.6° (c 0.16, $CHCl_3$); IR γ_{max} (film) 3547, 2925, 2853, 1723, 1368, 1275, 1236, 1099, 1070, 760, 712 cm^{-1}; ^1H NMR ($CDCl_3$) δ 1.51 (3H, s), 1.56 (3H, s), 1.60 (3H, s), 1.61 (3H, s), 1.73 (3H, s), 2.14 (3H, s), 2.10−2.30 (4H, m), 2.50 (1H, m), 2.98 (1H, s), 4.91 (1H, d, J = 6.8 Hz), 5.51 (1H, d, J = 3.6 Hz), 5.64 (1H, s), 5.78 (1H, m), 6.74 (1H, d, J = 1.1 Hz), 7.42 (1H, d, J = 1.1 Hz), 6.74 (2H, m), 7.57 (1H, m), 7.97 (2H, dd, J = 1.2, 7.0 Hz), 8.03 (1H, s); MS (EI) m/z (%) 569 (M^+ − 15, 1), 542 (1), 524 (3), 457 (4), 420 (3), 402 (22), 192 (26), 149 (100), 105 (86), 94 (51), 57 (47); HRMS (EI) m/z calcd for $C_{30}H_{33}O_{11}$ 569.20229, found 569.19952.

1α-Acetoxy-2α-benzoyloxy-9β-furoyloxy-6β-(*S*)-(+)-2-methylbutyroyloxy-4β-hydroxydihydro-β-agarofuran (24). Compound **22** (4.0 mg) was treated under the conditions already described for the synthesis of **15**, affording **24** (3.2 mg): colorless lacquer; $[\alpha]^{20}_D$ = +6.3° (c 0.3, $CHCl_3$); IR γ_{max} (film) 3553, 2924, 2854, 1727, 1462, 1273, 1144, 1098, 1071, 1026, 800, 712 cm^{-1}; ^1H NMR ($CDCl_3$) δ 0.91 (3H, t, J = 7.4 Hz), 1.20 (3H, d, J = 7.0 Hz), 1.51 (3H, s), 1.58 (6H, s), 1.62 (3H, s), 1.72 (3H, s), 1.74 (1H, m), 1.98−2.27 (4H, m), 2.44−2.50 (2H, m), 2.97 (1H, s), 4.92 (1H, d, J = 7.0 Hz), 5.52 (1H, d, J = 3.6 Hz), 5.69 (1H, s), 5.78 (1H, m), 6.73 (1H, s), 7.47 (3H, m), 7.58 (1H, m), 7.97 (2H, dd, J = 1.3, 7.0 Hz), 8.03 (1H, s); MS (EI) m/z (%) 611 (M^+ − 15, 4), 542 (2), 524 (1), 499 (7), 462 (1), 402 (43), 290 (8), 192 (25), 105 (100), 95 (66), 57 (83); HRMS (EI) m/z calcd for $C_{33}H_{39}O_{11}$ 611.24924, found 611.24674.

1α-Acetoxy-2α-benzoyloxy-9β-furoyloxy-6β-lauroyloxy-4β-hydroxydihydro-β-agarofuran (25). Compound **22** (6.0 mg) was treated under the conditions already described for the synthesis of **16**, affording **25** (4.3 mg): colorless lacquer; $[\alpha]^{20}_D$ = +27.5° (c 0.43, $CHCl_3$); IR γ_{max} (film) 3554, 2925, 2854, 1724, 1311, 1273, 1228, 1160, 1106, 1070, 762, 711 cm^{-1}; ^1H NMR ($CDCl_3$) δ 0.87 (3H, t, J = 6.2 Hz), 1.26 (14H, s), 1.51 (3H, s), 1.51−1.66 (4H, m), 1.56 (3H, s), 1.59 (3H, s), 1.67 (3H, s), 1.73 (3H, s), 2.15−2.50 (7H, m), 2.98 (1H, s), 4.92 (1H, d, J = 6.7 Hz), 5.51 (1H, d, J = 3.6 Hz), 5.66 (1H, s), 5.78 (1H, m), 6.74 (1H, t, J = 1.1 Hz), 7.46 (3H, m), 7.58 (1H, m), 7.97 (2H, dd, J = 1.2, 7.1 Hz), 8.03 (1H, t, J = 0.7 Hz); MS (EI) m/z (%) 709 (M^+ − 15, 4), 597 (7), 560 (1), 542 (1), 524 (3), 420 (6), 402 (56), 192 (4), 105 (100), 95 (59), 57 (32); HRMS (EI) m/z calcd for $C_{40}H_{53}O_{11}$ 709.35879, found 709.35315.

1α-Acetoxy-2α-benzoyloxy-9β-furoyloxy-6β-(1)-naphthoyloxy-4β-hydroxydihydro-β-agarofuran (26). Compound **22** (3.5 mg) was treated under the conditions already described for the synthesis of **17**, affording **26** (3.1 mg): colorless lacquer; $[\alpha]^{20}_D$ = +31.8° (c 0.28, $CHCl_3$); IR γ_{max} (film) 3434, 2924, 2853, 1724, 1366, 1277, 1244, 1134, 759, 712 cm^{-1}; ^1H NMR ($CDCl_3$) δ 1.55 (3H, s), 1.59 (3H, s), 1.70 (3H, s), 1.71 (3H, s), 1.75 (3H, s), 2.04−2.33 (4H, m), 2.66 (1H, m), 3.24 (1H, s), 5.01 (1H, d, J = 6.6 Hz), 5.58 (1H, d, J = 3.6 Hz), 5.84 (1H, m), 5.99 (1H, s), 6.76 (1H, d, J = 1.6 Hz), 7.46 (3H, m), 7.56 (2H, m), 7.65 (1H, m), 7.90 (2H, m), 7.97 (2H, m), 8.05 (3H, m), 8.72 (1H, d, J = 7.3 Hz), 9.20 (1H, d, J = 8.7 Hz); MS (EI)

m/z (%) 681 ($M^+ - 15$, 1), 569 (1), 533 (1), 420 (1), 402 (7), 155 (100), 127 (14), 105 (24); HRMS (EI) *m/z* calcd for $C_{39}H_{37}O_{11}$ 681.23359, found 681.23106.

1α-Acetoxy-2α-benzoyloxy-9β-furoyloxy-6β-pivayloxy-4β-hydroxydihydro-β-agarofuran (27). Compound **22** (3.0 mg) was treated under the conditions already described for the synthesis of **18**, affording **27** (2.9 mg): colorless lacquer; $[\alpha]^{20}_D = +40.8°$ (*c* 0.25, $CHCl_3$); IR γ_{max} (film) 3553, 2958, 2925, 2853, 1722, 1366, 1313, 1275, 1231, 1118, 1106, 1068, 1026, 760, 712 cm^{-1}; ^1H NMR ($CDCl_3$) δ 1.25 (9H, s), 1.51 (3H, s), 1.58 (6H, s), 1.62 (3H, s), 1.72 (3H, s), 2.10−2.27 (4H, m), 2.50 (1H, m), 2.94 (1H, s), 4.92 (1H, d, $J = 6.7$ Hz), 5.52 (1H, d, $J = 3.6$ Hz), 5.69 (1H, s), 5.79 (1H, m), 6.74 (1H, d, $J = 1.6$ Hz), 7.44 (3H, m), 7.58 (1H, m), 7.97 (2H, dd, $J = 1.3$, 7.4 Hz), 8.03 (1H, s); MS (EI) *m/z* (%) 611 ($M^+ - 15$, 1), 499 (3), 402 (26), 290 (6), 192 (8), 105 (100), 95 (54), 57 (63); HRMS (EI) *m/z* calcd for $C_{33}H_{39}O_{11}$ 611.24924, found 611.24870.

1α-Acetoxy-2α-benzoyloxy-9β-furoyloxy-6β-trifluoroacetoxy-4β-hydroxydihydro-β-agarofuran (28). Compound **22** (5.0 mg) was treated under the conditions already described for the synthesis of **19**, affording **28** (4.2 mg): colorless lacquer; $[\alpha]^{25}_D = +46.6°$ (*c* 0.36, $CHCl_3$); IR γ_{max} (film) 3448, 2926, 2851, 1775, 1726, 1369, 1271, 1223, 1174, 1142, 1095, 1038, 760, 711 cm^{-1}; ^1H NMR ($CDCl_3$) δ 1.51 (3H, s), 1.54 (3H, s), 1.67 (3H, s), 1.73 (3H, s), 2.07 (3H, s), 2.25−2.61 (4H, m), 3.29 (1H, dd, $J = 3.3$, 14.7 Hz), 4.96 (1H, d, $J = 6.6$ Hz), 5.63 (1H, d, $J = 3.8$ Hz), 5.73 (1H, s), 5.91 (1H, m), 6.74 (1H, d, $J = 1.6$ Hz), 7.45 (3H, m), 7.60 (1H, m), 7.94 (2H, dd, $J = 1.3$, 7.1 Hz), 8.04 (1H, s); MS (EI) *m/z* (%) 638 (M^+, 1), 623 (1), 499 (1), 457 (1), 363 (1), 345 (1), 307 (1), 289 (1), 231 (1), 173 (2), 137 (24), 105 (100), 95 (71); HRMS (EI) *m/z* calcd for $C_{30}H_{30}O_{11}F_3$ 623.17403, found 623.16983.

1α-Acetoxy-2α-benzoyloxy-9β-furoyloxy-6β-(4)-methoxybenzoyloxy-4β-hydroxydihydro-β-agarofuran (29). Compound **22** (3.0 mg) was treated with (4)-methoxybenzoyl chloride (0.1 mL) under the conditions already described for the synthesis of **18**, affording **29** (2.5 mg). Colorless lacquer; $[\alpha]^{20}_D = +18.3°$ (*c* 0.18, $CHCl_3$); IR γ_{max} (film) 3546, 2924, 2853, 1721, 1606, 1366, 1257, 1168, 1106, 1025, 760, 712 cm^{-1}; ^1H NMR ($CDCl_3$) δ 1.53 (3H, s), 1.57 (3H, s), 1.63 (3H, s), 1.65 (3H, s), 1.74 (3H, s), 2.20−2.38 (4H, m), 2.58 (1H, m), 3.18 (1H, s), 3.86 (3H, s), 4.96 (1H, d, $J = 6.3$ Hz), 5.55 (1H, d, $J = 3.6$ Hz), 5.76 (1H, s), 5.81 (1H, m), 6.75 (1H, d, $J = 1.4$ Hz), 6.96 (2H, dd, $J = 8.8$, 1.9 Hz), 7.43 (3H, m), 7.55 (1H, m), 7.96 (2H, dd, $J = 1.3$, 7.1 Hz), 8.04 (1H, s), 8.17 (2H, dd, $J = 8.8$, 1.9 Hz); MS (EI) *m/z* (%) 661 ($M^+ - 15$,1), 549 (2), 402 (11), 135 (100), 105 (18); HRMS (EI) *m/z* calcd for $C_{36}H_{37}O_{12}$ 661.22850, found 661.22408.

1α-Acetoxy-2α-benzoyloxy-9β-furoyloxy-6β-(4)-nitrobenzoyloxy-4β-hydroxydihydro-β-agarofuran (30). Compound **22** (6.0 mg) was treated with 4-nitrobenzoyl chloride (0.1 mL) under the conditions already described for the synthesis of **18**, affording **30** (4.7 mg): colorless lacquer; $[\alpha]^{20}_D = +26.5°$ (*c* 0.47, $CHCl_3$); IR γ_{max} (film) 3546, 2925, 2853, 1721, 1530, 1348, 1277, 1106, 1025, 760, 715 cm^{-1}; ^1H NMR ($CDCl_3$) δ 1.56 (6H, s), 1.63 (3H, s), 1.67 (3H, s), 1.75 (3H, s), 2.18−2.60 (5H, m), 4.98 (1H, d, $J = 6.7$ Hz), 5.56 (1H, d, $J = 3.6$ Hz), 5.82 (2H, m), 6.76 (1H, d, $J = 1.7$ Hz), 7.44 (3H, m), 7.57 (1H, m), 7.96 (2H, d, $J = 7.3$ Hz), 8.05 (1H, s), 8.31 (2H, m), 8.42 (2H, d, $J = 8.7$ Hz); MS (EI) *m/z* (%) 676 ($M^+ - 15$, 1), 564 (6), 402 (49), 290 (11), 192 (42), 150 (29), 120 (20), 105 (100), 95 (68), 77 (12); HRMS (EI) *m/z* calcd for $C_{35}H_{34}N_1O_{13}$ 676.20302, found 676.20139.

Biological Assays. 1. Parasite Culture. The wild-type (WT) *L. tropica* LRC-strain was a clone obtained by agar plating.[11] A *L. tropica* line highly resistant to DNM (MDR line) was maintained in the presence of 150 μM DNM and used as previously described.[6] This resistant line had an MDR phenotype similar to tumor cells, with a cross-resistance profile to several drugs and an overexpressed drug-efflux Pgp-like transporter.[6] Promastigote forms were grown at 28 °C in RPMI 1640-modified medium (Gibco) and supplemented with 20% heat-inactivated fetal bovine serum (Gibco).

2. DNM Chemosensitization Experiments. The viability of parasites in the presence of the different sesquiterpenes was analyzed by an MTT-based assay as previously described for *Leishmania*.[5] The screening was performed in flat-bottomed 96-well plastic plates maintained at 28 °C. Promastigote forms from a logarithmic phase culture were suspended in fresh medium to yield 6×10^6 cells/mL. Each well was filled with 50 μL of the parasite suspension (3×10^5 cells). Stock solutions of sesquiterpenes dissolved in DMSO were diluted directly in the culture medium at the suitable concentrations, and 50 μL was added to each well. The final DMSO content did not exceed 0.3%, which had no effect on parasite growth. To assess the chemosensitizing activity of sesquiterpenes, promastigotes of the *L. tropica* MDR line were exposed to both DNM (150 μM) and sesquiterpenes. To determine the intrinsic toxicity of the sesquiterpenes, the WT and MDR *L. tropica* lines were exposed to sesquiterpenes in the absence of DNM. After 72 h of incubation at 28 °C, the viability of promastigotes was determined by the colorimetric MTT assay. A 10-μL portion of 3-(4,5-dimethylthiazol-2-yl)-2,5-diphenyltetrazolium bromide (MTT) (5 mg/mL in PBS) was added to each well, and plates were incubated for an additional period of 4 h. Water-insoluble formazan crystals were dissolved by adding 100 μL of SDS 20%, and absorbance was read at 540 nm using a microplate reader (Beckman Biomek 2000). Cell survival was determined by dividing the absorbance at a given sesquiterpene concentration by the absorbance of control cells. The results are expressed as percent growth inhibition (GI). IC_{50} values, the concentration of DNM that decreases the rate of parasite growth by 50%, were determined for the WT and MDR lines. Resistance indexes were calculated as the IC_{50} ratio between the MDR and WT lines in the presence of different concentrations of sesquiterpenes.

3. Reversion of Calcein Accumulation in a MDR *L. tropica* Line Overexpressing a Pgp-Like Transporter. The accumulation of CAL fluorescent dye in the WT and MDR *Leishmania* lines was estimated by flow cytometry using a Becton Dickinson FacScan, as described.[5] Briefly, parasites were incubated with 2 μM CAL-acetoxymethyl ester (CAL-AM) (Molecular Probes Europe BV, The Netherlands), for 1 h at 28 °C in HPMI−glucose buffer (10 mM HEPES, 120 mM NaCl, 5 mM Na_2HPO_4, 0.4 mM $MgCl_2$, 0.04 mM $CaCl_2$, 10 mM $NaHCO_3$, 10 mM glucose, 5 mM KCl, pH 7.4), in the presence or in absence of different concentrations of sesquiterpenes. Parasites were then extensively washed, resuspended in cold phosphate-buffered saline (PBS; 1.2 mM KH_2PO_4, 8.1 mM Na_2HPO_4, 130 mM NaCl, 2.6 mM KCl adjusted to pH 7.4), and immediately analyzed. Cells were gated on the basis of size and complexity to eliminate dead cells and debris from the analysis. Quantification of intracellular fluorescence was carried out by scanning the emission between 515 and 545 nm (FL-1) using the Cell Quest Software application.

Acknowledgment. This work has been supported by the Spanish Grants PPQ2000-1655-C02-02, BQU2000-0870-CO2-01 and CICYT (SAF2003-02730). Some of the simulations were run at the Centre de Computació i Comunicacions de Catalunya. F.C.S. was a recipient of a fellowship (B.E.F.I. Exp. 00/9068) from the Fondo de Investigación Sanitaria, Instituto de Salud Carlos III, Ministerio de Sanidad y Consumo (Spain). We thank Pilar Navarro for her help in parasite culture. We would also like to acknowledge Pharmacia & Upjohn (Barcelona, Spain) for providing the DNM used in this study.

Supporting Information Available: IR, MS, HRMS, and ^1H NMR spectra for the compounds **11**−**30** described. This material is available free of charge via the Internet at http://pubs.acs.org.

References

(1) Nicolaou, K. C.; Pfefferkorn, J. A.; Roecker, A. J.; Cao, G. Q.; Barluenga, S.; Mitchell, H. J. Natural product-like combinatorial libraries based on privileged structures. 1. General principles and solid-phased synthesis of benzopyrans. *J. Am. Chem. Soc.* **2000**, *122*, 9939−9953

(2) Spivey, A. C.; Weston, M.; Woodhead, S. Celastraceae sesquiterpenoids: Biological activity and synthesis. *Chem. Soc. Rev.* **2002**, *31*, 43−59.

(3) Duan, H.; Takaishi, Y.; Momota, H.; Ohmoto, Y.; Taki, T.; Jia, Y.; Li, D. Immunosuppressive sesquiterpene alkaloids from *Tripterygium wilfordii*. *J. Nat. Prod.* **2001**, *64*, 582−587

(4) Duan, H.; Takaishi, Y.; Imakura, Y.; Jia, Y.; Duan, L.; Cosentino, M.; Lee, K. Sesquiterpene alkaloids from *Tripterygium hypoglaucum* and *Tripterygium wilfordii*: A new class of potent anti-HIV agents. *J. Nat. Prod.* **2000**, *63*, 357−361.

(5) Kennedy, M. L.; Cortés-Selva, F.; Pérez-Victoria, J. M.; Jiménez, I. A.; González, A. G.; Muñoz, O. M.; Gamarro, F.; Castanys, S.; Ravelo, A. G. Chemosensitization of a multidrug- resistant *Leishmania tropica* line by new sesquiterpenes from M*aytenus magellanica* and M*aytenus chubutensis*. *J. Med. Chem.* **2001**, *44*, 4668−4676.

(6) Pérez-Victoria, J. M.; Pérez-Victoria, F. J.; Parodi-Talice, A.; Jimenez, I. A.; Ravelo, A. G.; Castanys, S.; Gamarro, F. Alkyllysophospholipid resistance in multidrug-resistant *Leishmania tropica* and chemosensitization by a novel P-glycoprotein-like transporter modulator. *Antimicrob. Agents Chemother.* **2001**, *45*, 2468−2474.

(7) González, A. G.; Tincusi, B. M.; Bazzocchi, I. L.; Tokuda, H.; Nishino, H.; Konoshima, T.; Jiménez, I. A.; Ravelo, A. G. Antitumor promoting effects of sesquiterpenes from *Maytenus cuzcoina* (Celastraceae). *Bioorg. Med. Chem.* **2000**, *8*, 1773−1778.

(8) Evans, B. E.; Rittle, K. E.; Bock, M. G.; DiPardo, R. M.; Freidinger, R. M.; Whitter, W. L.; Lundell, G. F.; Veber, D. F.; Anderson, P. S.; Chang, R. S. L.; Lotti, V. J.; Cerino, D. J.; Chen, T. B.; Kling, P. J.; Kunkel, K. A.; Springer, J. P.; Hirshfield, J. Methods for drug discovery: Development of potent, selective, orally effective cholecystokinin antagonists. *J. Med. Chem.* **1988**, *31*, 2235−2246.

(9) Reed, M. B.; Saliba, K. J.; Caruana, S. R.; Kirk, K.; Cowman, A. F. Pgh1 modulates sensitivity and resistance to multiple antimalarials in *Plasmodium falciparum*. *Nature* **2000**, *403*, 906−909.

(10) Ouellette, M.; Legare, D.; Haimeur, A.; Grondin, K.; Roy, G.; Brochu, C.; Papadopoulou, B. ABC transporters in *Leishmania* and their role in drug resistance. *Drug Res. Updates* **1998**, *I*, 43−48.

(11) Chiquero, M. J.; Pérez-Victoria, J. M.; O'Valle, F.; González-Ros, J. M.; del Moral, R.; Ferragut, J. A.; Castanys, S.; Gamarro, F. Altered drug membrane permeability in a multidrug-resistant *Leishmania tropica* line. *Biochem. Pharmacol.* **1998**, *55*, 131−139.

(12) Kole, L.; Das, L.; Das, P. K. Synergistic effect on interferon-gamma and mannosylated liposome-incorporated doxorubicin in the therapy of experimented visceral leishmaniasis. *J. Infect. Dis.* **1999**, *180*, 811−820.

(13) Kapoor, P.; Sachdeva, M.; Madhubala, R. Effect of the microtubule stabilizing agent taxol on leishmanial protozoan parasites in vitro. FEMS *Microbiol. Lett.* **1999**, *176*, 429−435.

(14) Urbina, J. A. Lipid biosynthesis pathways as chemotherapeutic targets in kinetoplastid parasites. *Parasitology* **1997**, *114*, 91−99.

(15) Marsella, R.; Ruiz de Gopegui, R. Leishmaniasis: A re-emerging zoonosis. *Int. J. Dermatol.* **1998**, *37*, 801−814.

(16) Pérez-Victoria, J. M.; Parodi-Talice, A.; Torres, C.; Gamarro, F.; Castanys, S. ABC transporters in the protozoan parasite *Leishmania*. *Intern. Microbiol.* **2001**, *4*, 159−166.

(17) Pérez-Victoria, J. M.; Tincusi, B. M.; Jimenez, I. A.; Bazzocchi, I. L.; Gupta, M. P.; Castanys, S.; Gamarro, F.; Ravelo, A. G. New natural sesquiterpenes as modulators of daunomycin resistance in a multidrug-resistant *Leishmania tropica* line. *J. Med. Chem.* **1999**, *42*, 4388−4393.

(18) Green, S. M.; Marshall, G. R. 3D-QSAR: A current perspective. *Trends Pharmacol. Sci.* **1995**, *16*, 285−291.

(19) Cramer, R. D.; Patterson, D. E.; Bunce, J. D. Comparative Molecular Field Analysis (CoMFA). 1. Effect of shape on binding of steroids to carrier proteins. *J. Am. Chem. Soc.* **1988**, *110*, 5959−5967.

(20) Clark, M.; Cramer, R. D. I.; Jones, D. M.; Patterson, D. E.; Simeroth, P. E. Comparative Molecular Field Analysis (CoMFA). 2. Toward its use with 3D-structural databases. *Tetrahedron Comput. Methodol.* **1990**, *3*, 47−59.

(21) Klebe, G.; Abraham, U.; Mietzner, T. Molecular Similarity Indices in a Comparative Analysis (CoMSIA) of drug molecules to correlate and predict their biological activity. *J. Med. Chem.* **1994**, *37*, 4130−4146.

(22) Singh, U. C.; Kollman, P. A. An approach to computing electrostatic charges for molecules. *J. Comput. Chem.* **1984**, *5*, 129−145.

(23) Cornell, W. D.; Cieplak, P.; Bayly, C.; Gould, I. R.; Merz, K. M.; Ferguson, D. M.; Spellmeyer, D. C.; Fox, T.; Caldwell, J. W.; Kollman, P. A. A second generation force field for the simulation of proteins, nucleic acids, and organic molecules. *J. Am. Chem. Soc.* **1995**, *117*, 5179−5197.

(24) Hawkins, G. D.; Giesen, D. J.; Lynch, G. C.; Chambers, C. C.; Rossi, I.; Storer, J. W.; Li, J.; Zhu, T.; Winget, P.; Rinaldi, D.; Liotard, D. A.; Cramer, C. J.; Truhlar, D. G. *AMSOL 6.7.2;* University of Minnesota, Minneapolis, MN 55455-0431.

(25) Böhm, M.; Stürzebecher, J.; Klebe, G. Three-dimensional quantitative structure−activity relationship analyses using comparative molecular field analysis and comparative molecular similarity indices analysis to elucidate selectivity differences of inhibitors binding to trypsin, thrombin, and factor xa. *J. Med. Chem.* **1999**, *42*, 458−477.

(26) Dunn, W. J. I.; Wold, S.; Edlund, U.; Hellberg, S.; Gasteiger, J. Multivariate structure−activity relationships between data from a battery of biological tests and an ensemble of structure descriptors: The PLS method. *Quant. Struct.-Act. Relat.* **1984**, *3*, 131−137.

(27) Wold, S.; Ruhe, A.; Wold, H.; Dunn, W. J. I. The covariance problem in linear regression. The partial least squares (PLS) approach to generalizad inverses. *SIAM J. Sci. Stat. Comput.* **1984**, *5*, 735−743.

(28) Cramer, R. D.; Bunce, J. D.; Patterson, D. E. Crossvalidation, bootstrapping and partial least squares compared with multiple regression in conventional QSAR studies. *Quant. Struct.-Act. Relat.* **1988**, *7*, 18−25.

(29) Wold, S.; Albano, C.; Dunn, W. J. I.; Edlund, U.; Esbenson, W.; Geladi, P.; Hellberg, S.; Johansson, E.; Lindberg, W.; Sjöström, M. Multivariate data analysis in chemistry. In *Chemometrics: Mathematics and Statistics in Chemistry*; Kowalsky, B. R., Ed.; Reidel: Dordrecht, The Netherlands, 1984; pp 17−95.

(30) *SYBYL 6.6;* Tripos Inc., 1699 South Hanley Rd., St. Louis, MO, 63144.

(31) Frisch, M. J.; Trucks, G. W.; Schlegel, H. B.; Scuseria, G. E.; Robb, M. A.; Cheeseman, J. R.; Zakrzewski, V. G.; Montgomery, J. A.; Keith, T. A.; Petersson, G. A.; Raghavachari, K.; Al-Laham, A.; Stratmann, R. E.; Burant, J. C.; Dapprich, S.; Millam, J. M.; Daniels, A. D.; Kudin, K. N.; Strain, M. C.; Farkas, O.; Tomasi, J.; Barone, V.; Cossi, M.; Cammi, R.; Menucci, B.; Pomelli, C.; Adamo, C.; Clifford, S.; Ochterski, J.; Petersson, G. A.; Ayala, P. Y.; Cui, Q.; Morokuma, K.; Malick, D. K.; Rabuck, A. D.; Raghavachari, K.; Foresman, J. B.; Cioslowski, J.; Ortiz, J. V.; Stefanov, B. B.; Liu, G.; Liashenko, A.; Piskorz, P.; Komaromi, I.; Gomperts, R.; Martin, R. L.; Fox, D. J.; Keith, T.; Al-Laham, M. A.; Peng, C. Y.; Nanayakkara, A.; González, C.; Challacombe, M.; Gill, P. M. W.; Johnson, B. G.; Chen, W.; Wong, W.; Andres, J. L.; Head-Gordon, M.; Replogle, E. S.; Pople, J. A. *Gaussian 98*; Gaussian, Inc., Pittsburgh, PA, 1998.

(32) Steiner, T.; Koellner, G. Hydrogen bonds with π-acceptors in proteins: Frequencies and role in stabilizing local 3D structures. *J. Mol. Biol.* **2001**, *305*, 535−557.

JM0309699